

2.2 Function-space View

An alternative and equivalent way of reaching identical results to the previous section is possible by considering inference directly in function space. We use a Gaussian process (GP) to describe a distribution over functions. Formally:

Definition 2.1 A Gaussian process is a collection of random variables, any finite number of which have a joint Gaussian distribution. \square

Gaussian process

A Gaussian process is completely specified by its mean function and covariance function. We define mean function $m(\mathbf{x})$ and the covariance function $k(\mathbf{x}, \mathbf{x}')$ of a real process $f(\mathbf{x})$ as

covariance and
mean function

$$\begin{aligned} m(\mathbf{x}) &= \mathbb{E}[f(\mathbf{x})], \\ k(\mathbf{x}, \mathbf{x}') &= \mathbb{E}[(f(\mathbf{x}) - m(\mathbf{x}))(f(\mathbf{x}') - m(\mathbf{x}'))], \end{aligned} \quad (2.13)$$

and will write the Gaussian process as

$$f(\mathbf{x}) \sim \mathcal{GP}(m(\mathbf{x}), k(\mathbf{x}, \mathbf{x}')). \quad (2.14)$$

Usually, for notational simplicity we will take the mean function to be zero, although this need not be done, see section 2.7.

In our case the random variables represent the value of the function $f(\mathbf{x})$ at location \mathbf{x} . Often, Gaussian processes are defined over time, i.e. where the index set of the random variables is time. This is not (normally) the case in our use of GPs; here the index set \mathcal{X} is the set of possible inputs, which could be more general, e.g. \mathbb{R}^D . For notational convenience we use the (arbitrary) enumeration of the cases in the training set to identify the random variables such that $f_i \triangleq f(\mathbf{x}_i)$ is the random variable corresponding to the case (\mathbf{x}_i, y_i) as would be expected.

index set \equiv
input domain

A Gaussian process is defined as a collection of random variables. Thus, the definition automatically implies a *consistency* requirement, which is also sometimes known as the marginalization property. This property simply means that if the GP e.g. specifies $(y_1, y_2) \sim \mathcal{N}(\boldsymbol{\mu}, \Sigma)$, then it must also specify $y_1 \sim \mathcal{N}(\mu_1, \Sigma_{11})$ where Σ_{11} is the relevant submatrix of Σ , see eq. (A.6). In other words, examination of a larger set of variables does not change the distribution of the smaller set. Notice that the consistency requirement is automatically fulfilled if the covariance function specifies entries of the covariance matrix.⁵ The definition does not exclude Gaussian processes with finite index sets (which would be simply Gaussian *distributions*), but these are not particularly interesting for our purposes.

marginalization
property

finite index set

⁵Note, however, that if you instead specified e.g. a function for the entries of the *inverse* covariance matrix, then the marginalization property would no longer be fulfilled, and one could not think of this as a consistent collection of random variables—this would not qualify as a Gaussian process.

Bayesian linear model
is a Gaussian process

A simple example of a Gaussian process can be obtained from our Bayesian linear regression model $f(\mathbf{x}) = \phi(\mathbf{x})^\top \mathbf{w}$ with prior $\mathbf{w} \sim \mathcal{N}(\mathbf{0}, \Sigma_p)$. We have for the mean and covariance

$$\begin{aligned}\mathbb{E}[f(\mathbf{x})] &= \phi(\mathbf{x})^\top \mathbb{E}[\mathbf{w}] = 0, \\ \mathbb{E}[f(\mathbf{x})f(\mathbf{x}')] &= \phi(\mathbf{x})^\top \mathbb{E}[\mathbf{w}\mathbf{w}^\top] \phi(\mathbf{x}') = \phi(\mathbf{x})^\top \Sigma_p \phi(\mathbf{x}').\end{aligned}\tag{2.15}$$

Thus $f(\mathbf{x})$ and $f(\mathbf{x}')$ are jointly Gaussian with zero mean and covariance given by $\phi(\mathbf{x})^\top \Sigma_p \phi(\mathbf{x}')$. Indeed, the function values $f(\mathbf{x}_1), \dots, f(\mathbf{x}_n)$ corresponding to any number of input points n are jointly Gaussian, although if $N < n$ then this Gaussian is singular (as the joint covariance matrix will be of rank N).

In this chapter our running example of a covariance function will be the *squared exponential*⁶ (SE) covariance function; other covariance functions are discussed in chapter 4. The covariance function specifies the covariance between pairs of random variables

$$\text{cov}(f(\mathbf{x}_p), f(\mathbf{x}_q)) = k(\mathbf{x}_p, \mathbf{x}_q) = \exp\left(-\frac{1}{2}|\mathbf{x}_p - \mathbf{x}_q|^2\right).\tag{2.16}$$

Note, that the covariance between the *outputs* is written as a function of the *inputs*. For this particular covariance function, we see that the covariance is almost unity between variables whose corresponding inputs are very close, and decreases as their distance in the input space increases.

basis functions

It can be shown (see section 4.3.1) that the squared exponential covariance function corresponds to a Bayesian linear regression model with an infinite number of basis functions. Indeed for every positive definite covariance function $k(\cdot, \cdot)$, there exists a (possibly infinite) expansion in terms of basis functions (see Mercer’s theorem in section 4.3). We can also obtain the SE covariance function from the linear combination of an infinite number of Gaussian-shaped basis functions, see eq. (4.13) and eq. (4.30).

The specification of the covariance function implies a distribution over functions. To see this, we can draw samples from the distribution of functions evaluated at any number of points; in detail, we choose a number of input points,⁷ X_* and write out the corresponding covariance matrix using eq. (2.16) elementwise. Then we generate a random Gaussian vector with this covariance matrix

$$\mathbf{f}_* \sim \mathcal{N}(\mathbf{0}, K(X_*, X_*)),\tag{2.17}$$

and plot the generated values as a function of the inputs. Figure 2.2(a) shows three such samples. The generation of multivariate Gaussian samples is described in section A.2.

smoothness

In the example in Figure 2.2 the input values were equidistant, but this need not be the case. Notice that “informally” the functions look smooth. In fact the squared exponential covariance function is infinitely differentiable, leading to the process being infinitely mean-square differentiable (see section 4.1). We also see that the functions seem to have a characteristic length-scale,

characteristic
length-scale

⁶Sometimes this covariance function is called the Radial Basis Function (RBF) or Gaussian; here we prefer squared exponential.

⁷Technically, these input points play the rôle of *test inputs* and therefore carry a subscript asterisk; this will become clearer later when both training and test points are involved.

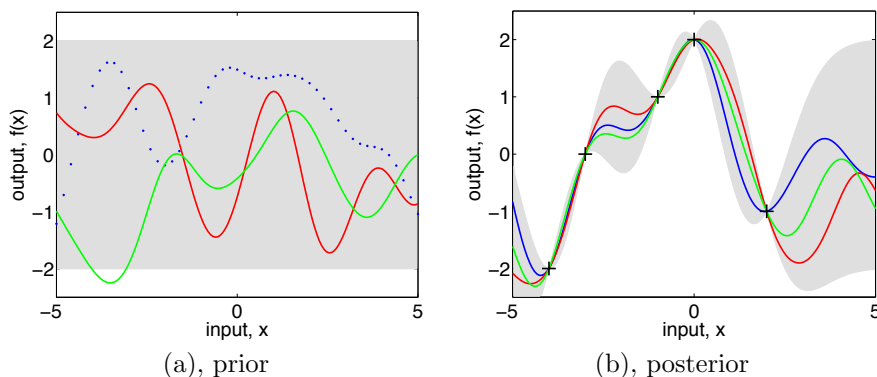


Figure 2.2: Panel (a) shows three functions drawn at random from a GP prior; the dots indicate values of y actually generated; the two other functions have (less correctly) been drawn as lines by joining a large number of evaluated points. Panel (b) shows three random functions drawn from the posterior, i.e. the prior conditioned on the five noise free observations indicated. In both plots the shaded area represents the pointwise mean plus and minus two times the standard deviation for each input value (corresponding to the 95% confidence region), for the prior and posterior respectively.

which informally can be thought of as roughly the distance you have to move in input space before the function value can change significantly, see section 4.2.1. For eq. (2.16) the characteristic length-scale is around one unit. By replacing $|\mathbf{x}_p - \mathbf{x}_q|$ by $|\mathbf{x}_p - \mathbf{x}_q|/\ell$ in eq. (2.16) for some positive constant ℓ we could change the characteristic length-scale of the process. Also, the overall variance of the random function can be controlled by a positive pre-factor before the exp in eq. (2.16). We will discuss more about how such factors affect the predictions in section 2.3, and say more about how to set such scale parameters in chapter 5.

magnitude

Prediction with Noise-free Observations

We are usually not primarily interested in drawing random functions from the prior, but want to incorporate the knowledge that the training data provides about the function. Initially, we will consider the simple special case where the observations are noise free, that is we know $\{(\mathbf{x}_i, f_i) | i = 1, \dots, n\}$. The joint distribution of the training outputs, \mathbf{f} , and the test outputs \mathbf{f}_* according to the prior is

joint prior

$$\begin{bmatrix} \mathbf{f} \\ \mathbf{f}_* \end{bmatrix} \sim \mathcal{N}\left(\mathbf{0}, \begin{bmatrix} K(X, X) & K(X, X_*) \\ K(X_*, X) & K(X_*, X_*) \end{bmatrix}\right). \quad (2.18)$$

If there are n training points and n_* test points then $K(X, X_*)$ denotes the $n \times n_*$ matrix of the covariances evaluated at all pairs of training and test points, and similarly for the other entries $K(X, X)$, $K(X_*, X_*)$ and $K(X_*, X)$. To get the posterior distribution over functions we need to restrict this joint prior distribution to contain only those functions which agree with the observed data points. Graphically in Figure 2.2 you may think of generating functions from the prior, and rejecting the ones that disagree with the observations, al-

graphical rejection

noise-free predictive
distribution

though this strategy would not be computationally very efficient. Fortunately, in probabilistic terms this operation is extremely simple, corresponding to *conditioning* the joint Gaussian prior distribution on the observations (see section A.2 for further details) to give

$$\mathbf{f}_*|X_*, X, \mathbf{f} \sim \mathcal{N}(K(X_*, X)K(X, X)^{-1}\mathbf{f}, K(X_*, X_*) - K(X_*, X)K(X, X)^{-1}K(X, X_*)). \quad (2.19)$$

Function values \mathbf{f}_* (corresponding to test inputs X_*) can be sampled from the joint posterior distribution by evaluating the mean and covariance matrix from eq. (2.19) and generating samples according to the method described in section A.2.

Figure 2.2(b) shows the results of these computations given the five data-points marked with + symbols. Notice that it is trivial to extend these computations to multidimensional inputs – one simply needs to change the evaluation of the covariance function in accordance with eq. (2.16), although the resulting functions may be harder to display graphically.

Prediction using Noisy Observations

It is typical for more realistic modelling situations that we do not have access to function values themselves, but only noisy versions thereof $y = f(\mathbf{x}) + \varepsilon$.⁸ Assuming additive independent identically distributed Gaussian noise ε with variance σ_n^2 , the prior on the noisy observations becomes

$$\text{cov}(y_p, y_q) = k(\mathbf{x}_p, \mathbf{x}_q) + \sigma_n^2 \delta_{pq} \quad \text{or} \quad \text{cov}(\mathbf{y}) = K(X, X) + \sigma_n^2 I, \quad (2.20)$$

where δ_{pq} is a Kronecker delta which is one iff $p = q$ and zero otherwise. It follows from the independence⁹ assumption about the noise, that a diagonal matrix¹⁰ is added, in comparison to the noise free case, eq. (2.16). Introducing the noise term in eq. (2.18) we can write the joint distribution of the observed target values and the function values at the test locations under the prior as

$$\begin{bmatrix} \mathbf{y} \\ \mathbf{f}_* \end{bmatrix} \sim \mathcal{N}\left(\mathbf{0}, \begin{bmatrix} K(X, X) + \sigma_n^2 I & K(X, X_*) \\ K(X_*, X) & K(X_*, X_*) \end{bmatrix}\right). \quad (2.21)$$

predictive distribution

Deriving the conditional distribution corresponding to eq. (2.19) we arrive at the key predictive equations for Gaussian process regression

$$\mathbf{f}_*|X, \mathbf{y}, X_* \sim \mathcal{N}(\bar{\mathbf{f}}_*, \text{cov}(\mathbf{f}_*)), \quad \text{where} \quad (2.22)$$

$$\bar{\mathbf{f}}_* \triangleq \mathbb{E}[\mathbf{f}_*|X, \mathbf{y}, X_*] = K(X_*, X)[K(X, X) + \sigma_n^2 I]^{-1}\mathbf{y}, \quad (2.23)$$

$$\text{cov}(\mathbf{f}_*) = K(X_*, X_*) - K(X_*, X)[K(X, X) + \sigma_n^2 I]^{-1}K(X, X_*). \quad (2.24)$$

⁸There are some situations where it is reasonable to assume that the observations are noise-free, for example for computer simulations, see e.g. [Sacks et al. \[1989\]](#).

⁹More complicated noise models with non-trivial covariance structure can also be handled, see section 9.2.

¹⁰Notice that the Kronecker delta is on the index of the cases, not the value of the input; for the signal part of the covariance function the input *value* is the index set to the random variables describing the function, for the noise part it is the *identity* of the point.

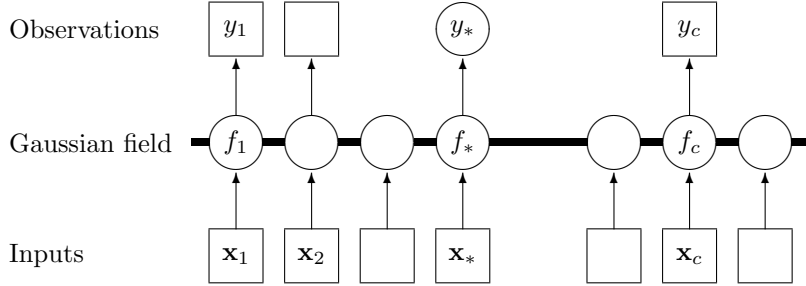


Figure 2.3: Graphical model (chain graph) for a GP for regression. Squares represent observed variables and circles represent unknowns. The thick horizontal bar represents a set of fully connected nodes. Note that an observation y_i is conditionally independent of all other nodes given the corresponding latent variable, f_i . Because of the marginalization property of GPs addition of further inputs, \mathbf{x} , latent variables, f , and *unobserved* targets, y_* , does not change the distribution of any other variables.

Notice that we now have exact correspondence with the weight space view in eq. (2.12) when identifying $K(C, D) = \Phi(C)^\top \Sigma_p \Phi(D)$, where C, D stand for either X or X_* . For any set of basis functions, we can compute the corresponding covariance function as $k(\mathbf{x}_p, \mathbf{x}_q) = \phi(\mathbf{x}_p)^\top \Sigma_p \phi(\mathbf{x}_q)$; conversely, for every (positive definite) covariance function k , there exists a (possibly infinite) expansion in terms of basis functions, see section 4.3.

correspondence with weight-space view

The expressions involving $K(X, X)$, $K(X, X_*)$ and $K(X_*, X_*)$ etc. can look rather unwieldy, so we now introduce a compact form of the notation setting $K = K(X, X)$ and $K_* = K(X, X_*)$. In the case that there is only one test point \mathbf{x}_* we write $\mathbf{k}(\mathbf{x}_*) = \mathbf{k}_*$ to denote the vector of covariances between the test point and the n training points. Using this compact notation and for a single test point \mathbf{x}_* , equations 2.23 and 2.24 reduce to

compact notation

$$\bar{f}_* = \mathbf{k}_*^\top (K + \sigma_n^2 I)^{-1} \mathbf{y}, \quad (2.25)$$

$$\mathbb{V}[f_*] = k(\mathbf{x}_*, \mathbf{x}_*) - \mathbf{k}_*^\top (K + \sigma_n^2 I)^{-1} \mathbf{k}_*. \quad (2.26)$$

Let us examine the predictive distribution as given by equations 2.25 and 2.26. Note first that the mean prediction eq. (2.25) is a linear combination of observations \mathbf{y} ; this is sometimes referred to as a *linear predictor*. Another way to look at this equation is to see it as a linear combination of n kernel functions, each one centered on a training point, by writing

predictive distribution

linear predictor

$$\bar{f}(\mathbf{x}_*) = \sum_{i=1}^n \alpha_i k(\mathbf{x}_i, \mathbf{x}_*) \quad (2.27)$$

where $\boldsymbol{\alpha} = (K + \sigma_n^2 I)^{-1} \mathbf{y}$. The fact that the mean prediction for $f(\mathbf{x}_*)$ can be written as eq. (2.27) despite the fact that the GP can be represented in terms of a (possibly infinite) number of basis functions is one manifestation of the *representer theorem*; see section 6.2 for more on this point. We can understand this result intuitively because although the GP defines a joint Gaussian distribution over all of the y variables, one for each point in the index set \mathcal{X} , for

representer theorem

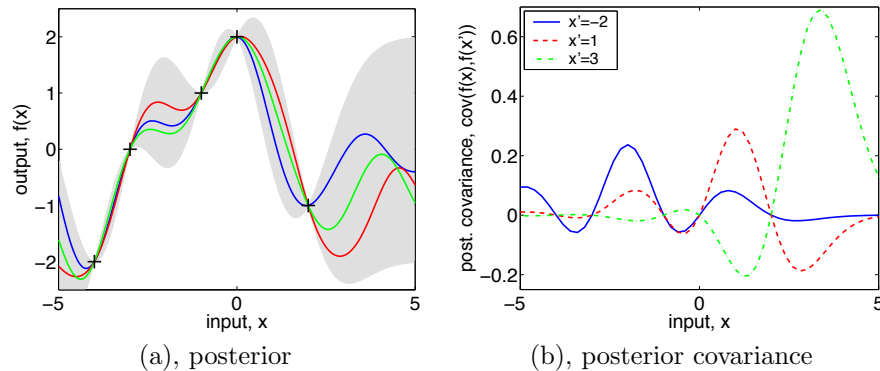


Figure 2.4: Panel (a) is identical to Figure 2.2(b) showing three random functions drawn from the posterior. Panel (b) shows the posterior *co*-variance between $f(\mathbf{x})$ and $f(\mathbf{x}')$ for the same data for three different values of \mathbf{x}' . Note, that the covariance at close points is high, falling to zero at the training points (where there is no variance, since it is a noise-free process), then becomes negative, etc. This happens because if the smooth function happens to be less than the mean on one side of the data point, it tends to exceed the mean on the other side, causing a reversal of the sign of the covariance at the data points. Note for contrast that the *prior* covariance is simply of Gaussian shape and never negative.

making predictions at \mathbf{x}_* we only care about the $(n+1)$ -dimensional distribution defined by the n training points and the test point. As a Gaussian distribution is marginalized by just taking the relevant block of the joint covariance matrix (see section A.2) it is clear that conditioning this $(n+1)$ -dimensional distribution on the observations gives us the desired result. A graphical model representation of a GP is given in Figure 2.3.

Note also that the variance in eq. (2.24) does not depend on the observed targets, but only on the inputs; this is a property of the Gaussian distribution. The variance is the difference between two terms: the first term $K(X_*, X_*)$ is simply the prior covariance; from that is subtracted a (positive) term, representing the information the observations gives us about the function. We can very simply compute the predictive distribution of test targets \mathbf{y}_* by adding $\sigma_n^2 I$ to the variance in the expression for $\text{cov}(\mathbf{f}_*)$.

The predictive distribution for the GP model gives more than just pointwise errorbars of the simplified eq. (2.26). Although not stated explicitly, eq. (2.24) holds unchanged when X_* denotes multiple test inputs; in this case the *co*-variance of the test targets are computed (whose diagonal elements are the pointwise variances). In fact, eq. (2.23) is the mean function and eq. (2.24) the covariance function of the (Gaussian) posterior process; recall the definition of Gaussian process from page 13. The posterior covariance is illustrated in Figure 2.4(b).

It will be useful (particularly for chapter 5) to introduce the *marginal likelihood* (or evidence) $p(\mathbf{y}|X)$ at this point. The marginal likelihood is the integral

noisy predictions

joint predictions

posterior process

marginal likelihood

input: X (inputs), \mathbf{y} (targets), k (covariance function), σ_n^2 (noise level), \mathbf{x}_* (test input) 2: $L := \text{cholesky}(K + \sigma_n^2 I)$ $\boldsymbol{\alpha} := L^\top \backslash (L \backslash \mathbf{y})$ 4: $\bar{f}_* := \mathbf{k}_*^\top \boldsymbol{\alpha}$ $\mathbf{v} := L \backslash \mathbf{k}_*$ 6: $\mathbb{V}[f_*] := k(\mathbf{x}_*, \mathbf{x}_*) - \mathbf{v}^\top \mathbf{v}$ $\log p(\mathbf{y} X) := -\frac{1}{2} \mathbf{y}^\top \boldsymbol{\alpha} - \sum_i \log L_{ii} - \frac{n}{2} \log 2\pi$ 8: return: \bar{f}_* (mean), $\mathbb{V}[f_*]$ (variance), $\log p(\mathbf{y} X)$ (log marginal likelihood)	} predictive mean eq. (2.25) } predictive variance eq. (2.26) eq. (2.30)
---	--

Algorithm 2.1: Predictions and log marginal likelihood for Gaussian process regression. The implementation addresses the matrix inversion required by eq. (2.25) and (2.26) using Cholesky factorization, see section A.4. For multiple test cases lines 4-6 are repeated. The log determinant required in eq. (2.30) is computed from the Cholesky factor (for large n it may not be possible to represent the determinant itself). The computational complexity is $n^3/6$ for the Cholesky decomposition in line 2, and $n^2/2$ for solving triangular systems in line 3 and (for each test case) in line 5.

of the likelihood times the prior

$$p(\mathbf{y}|X) = \int p(\mathbf{y}|\mathbf{f}, X) p(\mathbf{f}|X) d\mathbf{f}. \quad (2.28)$$

The term *marginal* likelihood refers to the marginalization over the function values \mathbf{f} . Under the Gaussian process model the prior is Gaussian, $\mathbf{f}|X \sim \mathcal{N}(\mathbf{0}, K)$, or

$$\log p(\mathbf{f}|X) = -\frac{1}{2} \mathbf{f}^\top K^{-1} \mathbf{f} - \frac{1}{2} \log |K| - \frac{n}{2} \log 2\pi, \quad (2.29)$$

and the likelihood is a factorized Gaussian $\mathbf{y}|\mathbf{f} \sim \mathcal{N}(\mathbf{f}, \sigma_n^2 I)$ so we can make use of equations A.7 and A.8 to perform the integration yielding the log marginal likelihood

$$\log p(\mathbf{y}|X) = -\frac{1}{2} \mathbf{y}^\top (K + \sigma_n^2 I)^{-1} \mathbf{y} - \frac{1}{2} \log |K + \sigma_n^2 I| - \frac{n}{2} \log 2\pi. \quad (2.30)$$

This result can also be obtained directly by observing that $\mathbf{y} \sim \mathcal{N}(\mathbf{0}, K + \sigma_n^2 I)$.

A practical implementation of Gaussian process regression (GPR) is shown in Algorithm 2.1. The algorithm uses Cholesky decomposition, instead of directly inverting the matrix, since it is faster and numerically more stable, see section A.4. The algorithm returns the predictive mean and variance for noise free test data—to compute the predictive distribution for noisy test data y_* , simply add the noise variance σ_n^2 to the predictive variance of f_* .

2.3 Varying the Hyperparameters

Typically the covariance functions that we use will have some free parameters. For example, the squared-exponential covariance function in one dimension has the following form

$$k_y(x_p, x_q) = \sigma_f^2 \exp\left(-\frac{1}{2\ell^2}(x_p - x_q)^2\right) + \sigma_n^2 \delta_{pq}. \quad (2.31)$$

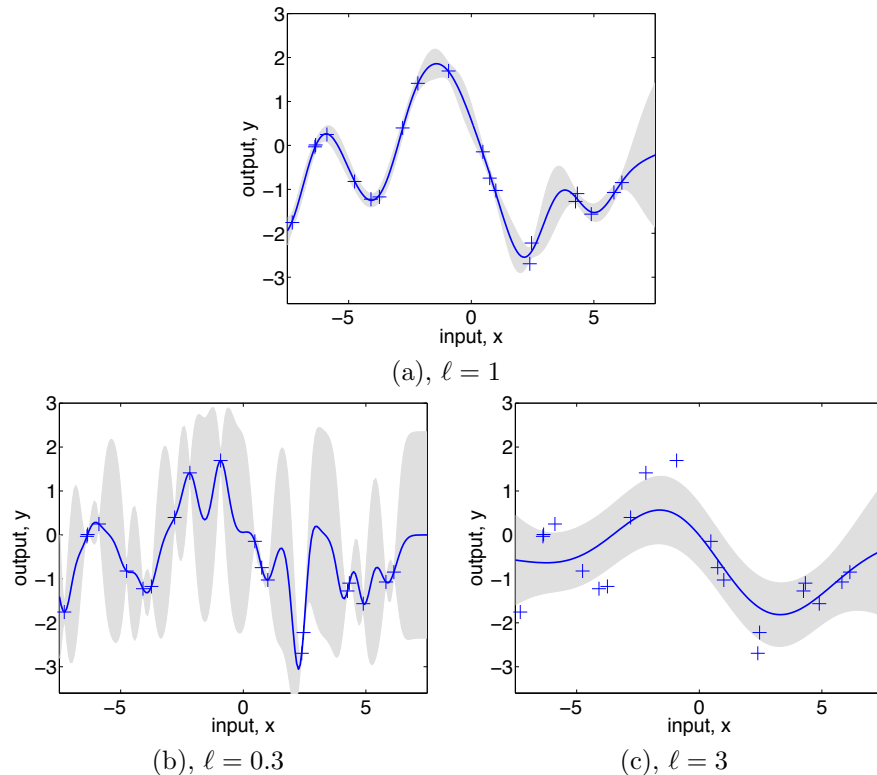


Figure 2.5: (a) Data is generated from a GP with hyperparameters $(\ell, \sigma_f, \sigma_n) = (1, 1, 0.1)$, as shown by the + symbols. Using Gaussian process prediction with these hyperparameters we obtain a 95% confidence region for the underlying function f (shown in grey). Panels (b) and (c) again show the 95% confidence region, but this time for hyperparameter values $(0.3, 1.08, 0.00005)$ and $(3.0, 1.16, 0.89)$ respectively.

hyperparameters

The covariance is denoted k_y as it is for the noisy targets y rather than for the underlying function f . Observe that the length-scale ℓ , the signal variance σ_f^2 and the noise variance σ_n^2 can be varied. In general we call the free parameters *hyperparameters*.¹¹

In chapter 5 we will consider various methods for determining the hyperparameters from training data. However, in this section our aim is more simply to explore the effects of varying the hyperparameters on GP prediction. Consider the data shown by + signs in Figure 2.5(a). This was generated from a GP with the SE kernel with $(\ell, \sigma_f, \sigma_n) = (1, 1, 0.1)$. The figure also shows the 2 standard-deviation error bars for the predictions obtained using these values of the hyperparameters, as per eq. (2.24). Notice how the error bars get larger for input values that are distant from any training points. Indeed if the x-axis

¹¹We refer to the parameters of the covariance function as hyperparameters to emphasize that they are parameters of a non-parametric model; in accordance with the weight-space view, section 2.1, the parameters (weights) of the underlying parametric model have been integrated out.

were extended one would see the error bars reflect the prior standard deviation of the process σ_f away from the data.

If we set the length-scale shorter so that $\ell = 0.3$ and kept the other parameters the same, then generating from this process we would expect to see plots like those in Figure 2.5(a) except that the x-axis should be rescaled by a factor of 0.3; equivalently if the same x-axis was kept as in Figure 2.5(a) then a sample function would look much more wiggly.

If we make predictions with a process with $\ell = 0.3$ on the data generated from the $\ell = 1$ process then we obtain the result in Figure 2.5(b). The remaining two parameters were set by optimizing the marginal likelihood, as explained in chapter 5. In this case the noise parameter is reduced to $\sigma_n = 0.00005$ as the greater flexibility of the “signal” means that the noise level can be reduced. This can be observed at the two datapoints near $x = 2.5$ in the plots. In Figure 2.5(a) ($\ell = 1$) these are essentially explained as a similar function value with differing noise. However, in Figure 2.5(b) ($\ell = 0.3$) the noise level is very low, so these two points have to be explained by a sharp variation in the value of the underlying function f . Notice also that the short length-scale means that the error bars in Figure 2.5(b) grow rapidly away from the datapoints.

too short length-scale

In contrast, we can set the length-scale longer, for example to $\ell = 3$, as shown in Figure 2.5(c). Again the remaining two parameters were set by optimizing the marginal likelihood. In this case the noise level has been increased to $\sigma_n = 0.89$ and we see that the data is now explained by a slowly varying function with a lot of noise.

too long length-scale

Of course we can take the position of a quickly-varying signal with low noise, or a slowly-varying signal with high noise to extremes; the former would give rise to a white-noise process model for the signal, while the latter would give rise to a constant signal with added white noise. Under both these models the datapoints produced should look like white noise. However, studying Figure 2.5(a) we see that white noise is not a convincing model of the data, as the sequence of y 's does not alternate sufficiently quickly but has correlations due to the variability of the underlying function. Of course this is relatively easy to see in one dimension, but methods such as the marginal likelihood discussed in chapter 5 generalize to higher dimensions and allow us to score the various models. In this case the marginal likelihood gives a clear preference for $(\ell, \sigma_f, \sigma_n) = (1, 1, 0.1)$ over the other two alternatives.

model comparison

2.4 Decision Theory for Regression

In the previous sections we have shown how to compute predictive distributions for the outputs y_* corresponding to the novel test input \mathbf{x}_* . The predictive distribution is Gaussian with mean and variance given by eq. (2.25) and eq. (2.26). In practical applications, however, we are often forced to make a decision about how to act, i.e. we need a point-like prediction which is optimal in some sense. To this end we need a *loss function*, $\mathcal{L}(y_{\text{true}}, y_{\text{guess}})$, which specifies the loss (or

optimal predictions
loss function